

Supplementary Materials for “The benefits of ambitious short-term targets when decarbonising the coupled electricity and heating energy system in Europe”

1. Historical Greenhouse Gases emissions in the European Union

The carbon budget from now onwards for the generation of electricity and the supply of heating in residential and services sector in Europe accounts for 21 GtCO₂. It has been estimated based on a global carbon budget of 800 GtCO₂ to avoid temperature increments above 2°C relative to preindustrial period with a probability of greater than 66% [1, 2]. The global budget is assumed to be split among regions according to a constant per-capita ratio which translates into a 6% share for Europe [3]. Out of the total emissions in Europe, the ratio corresponding to electricity and heating is considered constant and equal to present values. In 2017, electricity generation and heating in the residential and services sector emitted 1.56 GtCO₂ which represents 43.5% of European emissions, [4] and Figure 1.

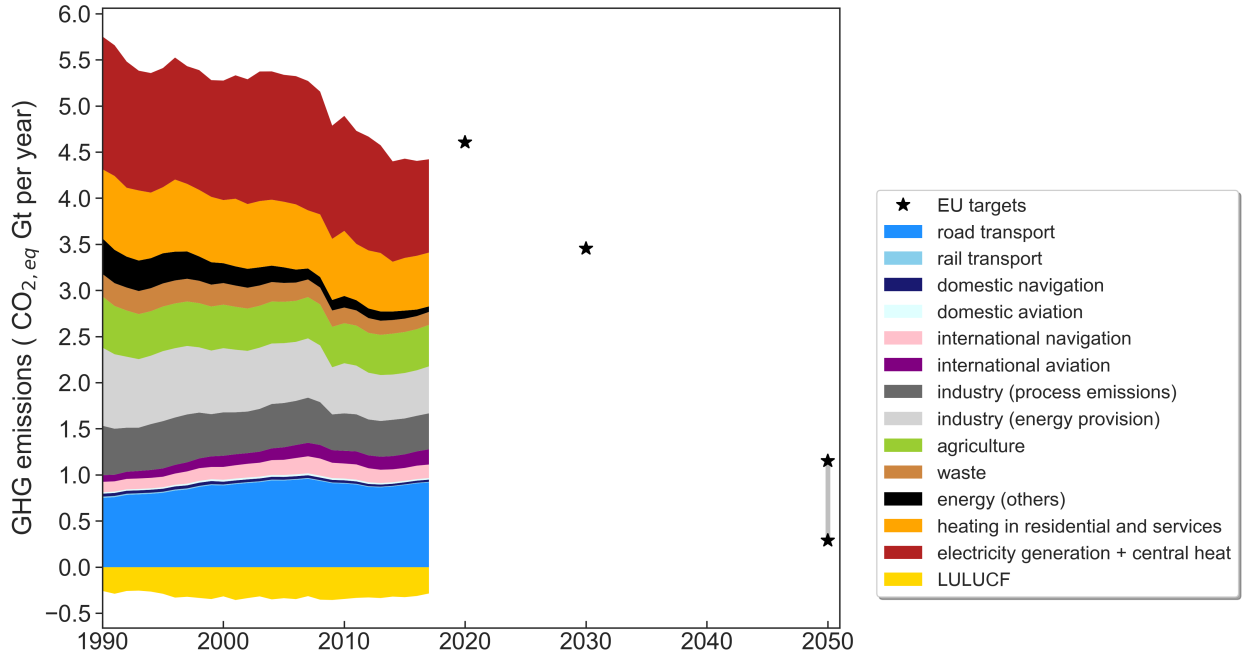


Figure 1: Sectoral distribution of historical emissions in the European Union [4]. The stars indicate committed EU reduction targets.

2. CO₂ restriction paths with equivalent budget

The $B=21$ GtCO₂ budget can be utilised following different transition paths. One option consists in assuming a linear CO₂ restriction path. Emissions will then reach zero in t_f

$$t_f = t_0 + \frac{2B}{e_0} \quad (1)$$

where $t_0=2020$, and e_0 represents the carbon emissions from electricity and heating sector in 2020, which are assumed to be the same as in 2017.

Alternatively, emissions can be assumed to follow a path defined by one minus the cumulative distribution function (CDF_β) of a beta distribution in which $\beta_1 = \beta_2$.

$$\begin{aligned} e(t) &= e_0(1 - CDF_\beta(t)) \\ CDF_\beta(t) &= \int_{-\infty}^t PDF_\beta(t)dt \\ PDF_\beta(t) &= \frac{\Gamma(\beta_1 + \beta_2)}{\Gamma(\beta_1) + \Gamma(\beta_2)} t^{\beta_1-1} (1-t)^{\beta_2-1} \end{aligned} \quad (2)$$

where Γ is the gamma function. The cumulative emissions fulfil $\int_{t_0}^{\infty} e(t)dt = B$.

The third option considered for the transition path is an exponential decay, following Raupach *et al.* [3]. In that case, emissions evolve as:

$$e(t) = e_0(1 + (r + m)t)e^{-mt} \quad (3)$$

where r is the initial linear growth rate, which here is assumed to be $r=0$, and the decay parameter m is determined by imposing the integral of the path to be equal to the budget.

$$\begin{aligned} B &= \int_{t_0}^{\infty} e_0(1 + (r + m)t)e^{-mt} dt \\ m &= \frac{1 + \sqrt{1 + \frac{rB}{e_0}}}{\frac{B}{e_0}} \end{aligned} \quad (4)$$

Although the exponential decay path approaches asymptotically to zero, we assume here that $e(2050) = 0$. By doing that, the final point of the different transition paths is equivalent and all of them achieve net-zero emissions by 2050.

3. Historical evolution of CO₂ emissions from heating supply in residential and services sector in European countries
4. Power plants in operation in Europe
5. Historical build rates for solar photovoltaics in European countries
6. Transition paths cautious and last-minute. Additional results

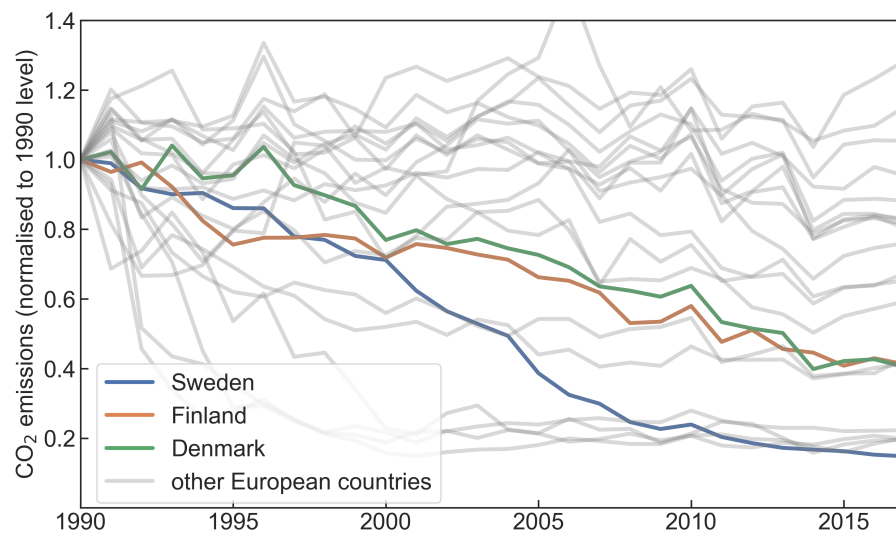


Figure 2: Historical CO₂ emissions from heating in residential and services sector [4].

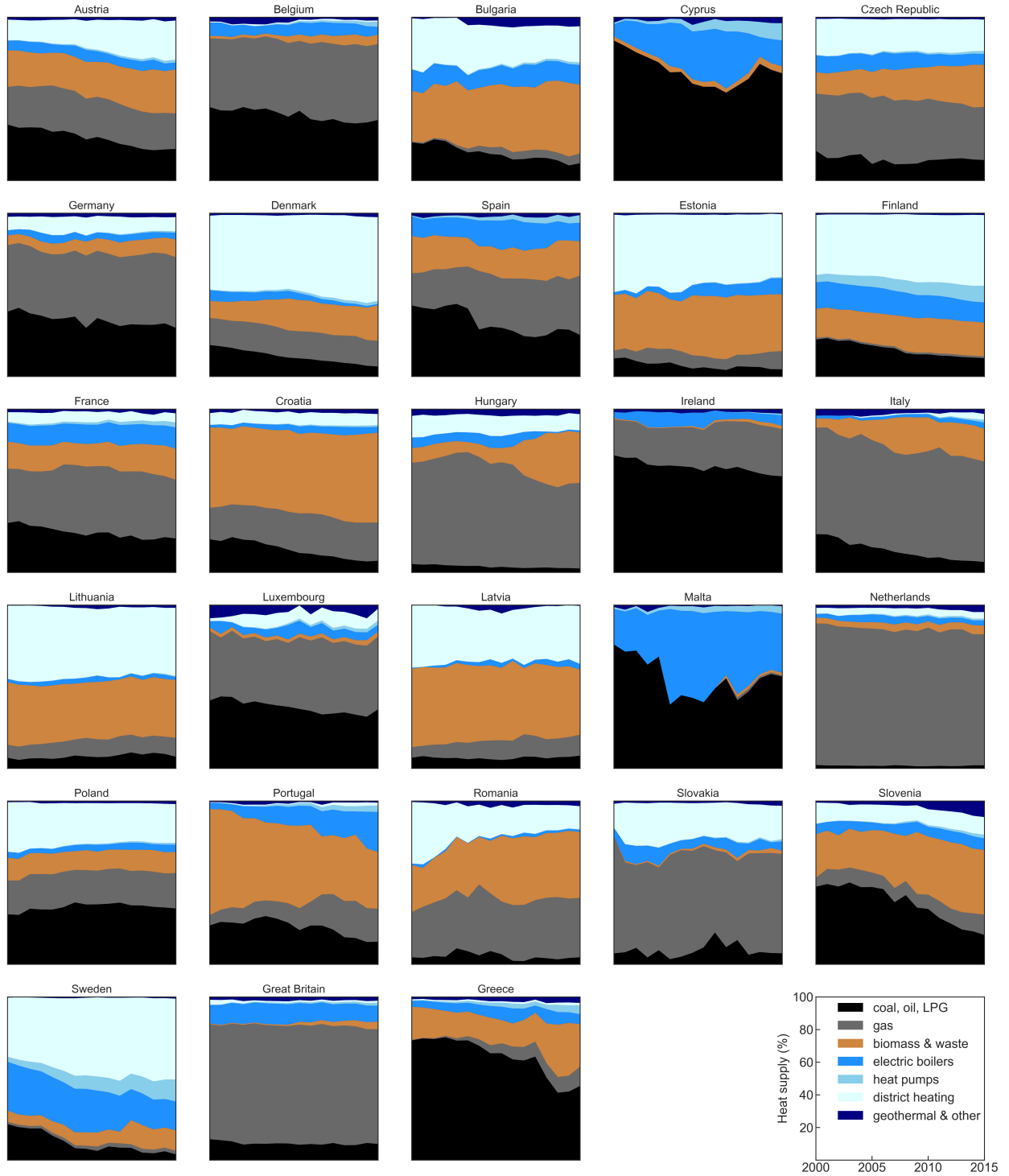


Figure 3: Historical share of technologies used to supply heating in residential and services sector [5].

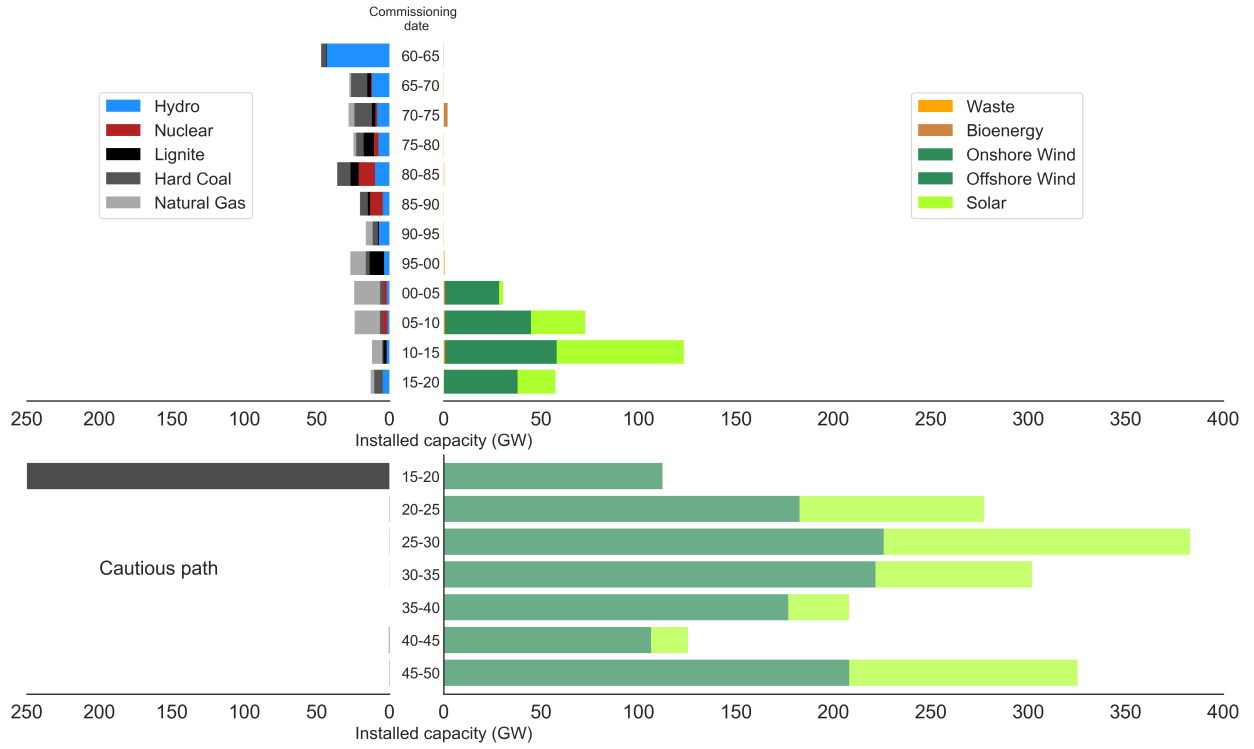


Figure 4: Age distribution of European power plants in operation[6, 7]

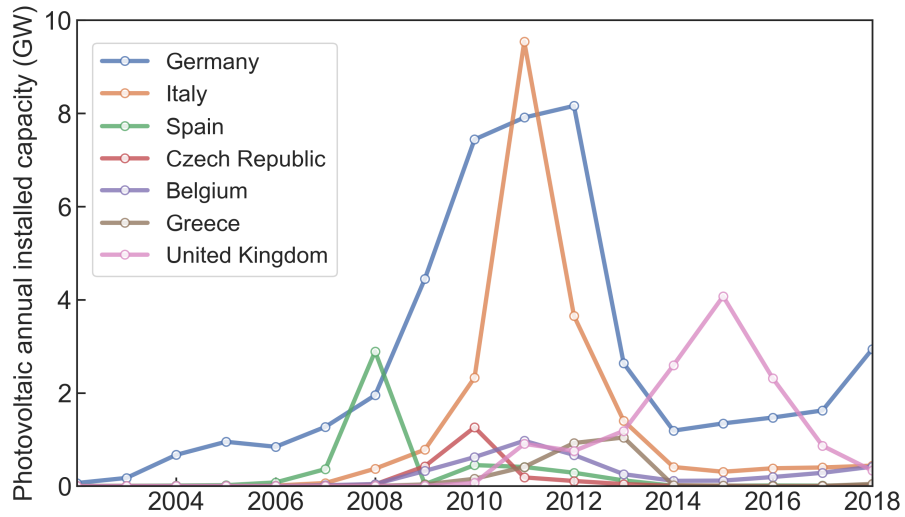


Figure 5: Photovoltaic annual build rates for those European countries with a prominent peak [7]. The sharp increase and subsequent decrease in the installation rates were caused by country-specific successive changes in the regulatory frameworks. See for instance [8, 9].

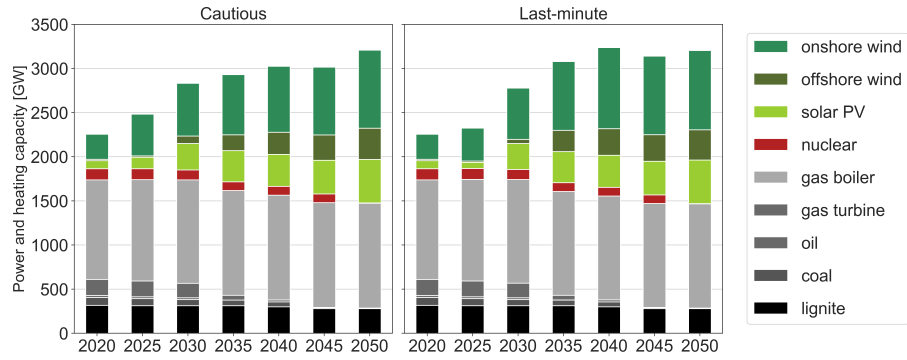


Figure 6: Installed capacities for different technologies throughout transition paths cautious and last-minute shown in Fig. 1 in the main text.

Figure 7: Primary energy in every country in 2050. (left) Cautious transition path, (right) Greenfield optimization for 2050.

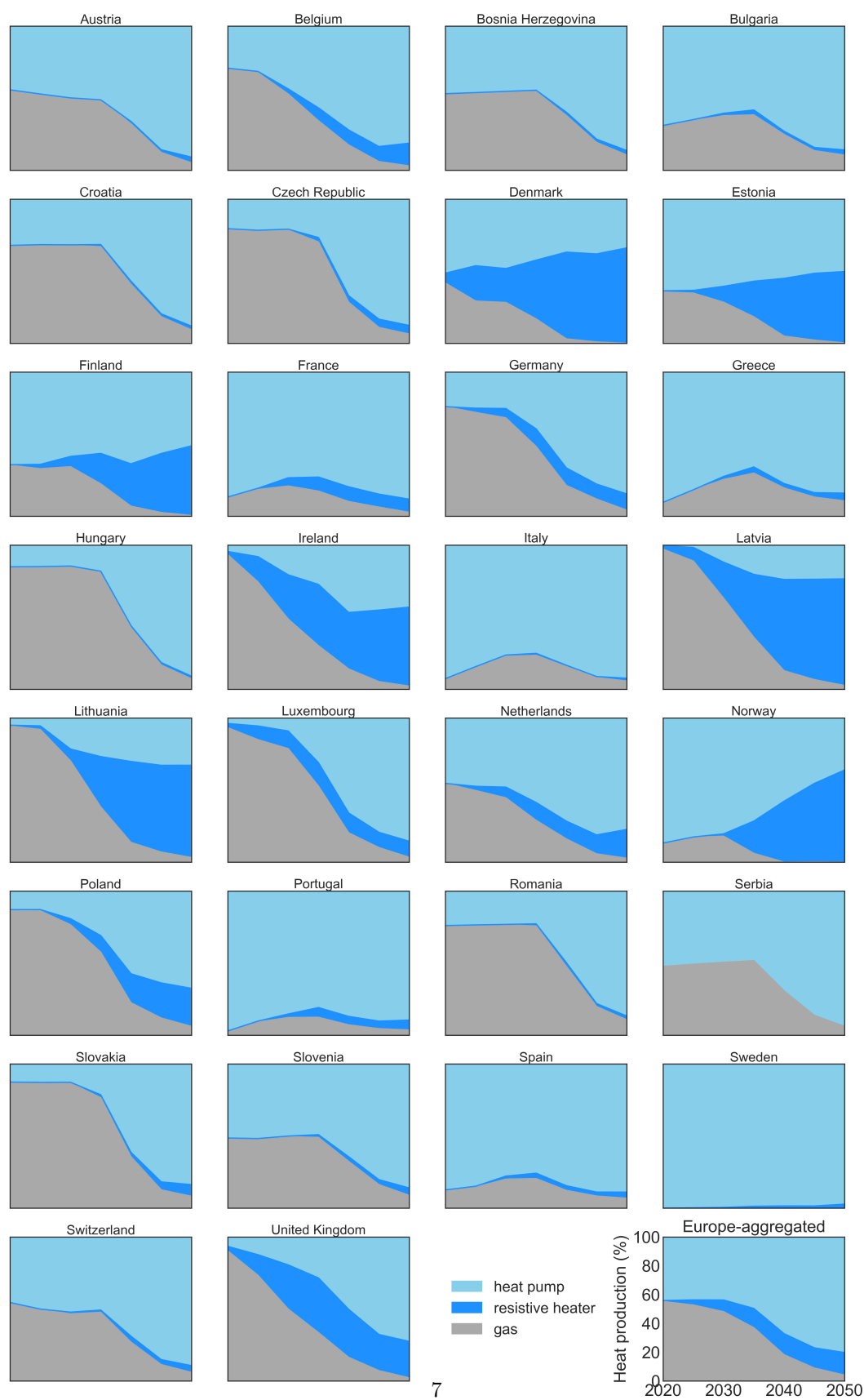


Figure 8: Evolution of technologies used to supply heating in residential and services sector in the cautious path.

7. Model description

In every time step, the optimisation objective, that is, the total annualised system cost is calculated as:

$$\min_{\substack{G_{n,s}, E_{n,s}, \\ F_\ell, g_{n,s,t}}} \left[\sum_{n,s} c_{n,s} \cdot G_{n,s} + \sum_{n,s} \hat{c}_{n,s} \cdot E_{n,s} + \sum_{\ell} c_\ell \cdot F_\ell + \sum_{n,s,t} o_{n,s,t} \cdot g_{n,s,t} \right] \quad (5)$$

where $c_{n,s}$ are the fixed annualised costs for generator and storage power capacity $G_{n,s}$ of technology s in every bus n , $\hat{c}_{n,s}$ are the fixed annualised costs for storage energy capacity $E_{n,s}$, c_ℓ are the fixed annualised costs for bus connectors F_ℓ , and $o_{n,s,t}$ are the variable costs (which in some cases include CO₂ tax), for generation and storage dispatch $g_{n,s,t}$ in every hour t . Bus connectors ℓ include transmission lines but also converters between the buses implemented in every country (see Figure ??), for instance, heat pumps that connect the electricity and heating bus.

The optimisation of the system is subject to several constraints. First, hourly demand $d_{n,t}$ in every bus n must be supplied by generators in that bus or imported from other buses. $f_{\ell,t}$ represents the energy flow on the link ℓ and $\alpha_{n,\ell,t}$ indicates both the direction and the efficiency of flow on the bus connectors. $\alpha_{n,\ell,t}$ can be time dependent such as in the case of heat pumps whose conversion efficiency depends on the ambient temperature.

$$\sum_s g_{n,s,t} + \sum_\ell \alpha_{n,\ell,t} \cdot f_{\ell,t} = d_{n,t} \leftrightarrow \lambda_{n,t} \quad \forall n, t \quad (6)$$

The Lagrange multiplier $\lambda_{n,t}$, also known as Karun-Kush-Tucker (KKT), associated with the demand constraint indicates the marginal price of the energy carrier in the bus n , *e.g.*, local marginal electricity price in the electricity bus.

Second, the maximum power flowing through the links is limited by their maximum physical capacity F_ℓ . For transmission links, $\underline{f}_{\ell,t} = -1$ and $\bar{f}_{\ell,t} = 1$, which allows both import and export between neighbouring countries. For a unidirectional converter *e.g.*, a heat resistor, $\underline{f}_{\ell,t} = 0$ and $\bar{f}_{\ell,t} = 1$ since a heat resistor can only convert electricity into heat.

$$\underline{f}_{\ell,t} \cdot F_\ell \leq f_{\ell,t} \leq \bar{f}_{\ell,t} \cdot F_\ell \quad \forall \ell, t. \quad (7)$$

For interconnecting transmission lines, the lengths l_ℓ are set by the distance between the geographical mid-points of each country, so that some of the transmission within each country is also reflected in the optimisation. A factor of 25% is added to the line lengths to account for the fact that transmission lines cannot be placed as the crow flies due to land use restriction. For the transmission lines capacities F_ℓ , a safety margin of 33% of the installed capacity is used to satisfy n-1 requirements [10].

Third, for every hour the maximum capacity that can provide a generator or storage is bounded by the product between installed capacity $G_{n,s}$ and availabilities $\underline{g}_{n,s,t}$, $\bar{g}_{n,s,t}$. For instance, for solar generators $\underline{g}_{n,s,t}$ is zero and $\bar{g}_{n,s,t}$ refers to the capacity factor at time t

$$\underline{g}_{n,s,t} \cdot G_{n,s} \leq g_{n,s,t} \leq \bar{g}_{n,s,t} \cdot G_{n,s} \quad \forall n, s, t. \quad (8)$$

The maximum power capacity for generators is limited by potentials $\bar{G}_{n,s}$ that are estimated taking into account physical and environmental constraints:

$$0 \leq G_{n,s} \leq \bar{G}_{n,s} \quad \forall n, s. \quad (9)$$

The storage technologies have a charging efficiency η_{in} and rate $g_{n,s,t}^+$, a discharging efficiency η_{out} and rate $g_{n,s,t}^-$, possible inflow $g_{n,s,t,\text{inflow}}$ and spillage $g_{n,s,t,\text{spillage}}$, and standing loss η_0 . The state of charge $e_{n,s,t}$ of every storage has to be consistent with charging and discharging in every hour and is limited by the energy capacity of the storage $E_{n,s}$. It should be remarked that the storage energy capacity $E_{n,s}$ can be optimised independently of the storage power capacity $G_{n,s}$.

$$\begin{aligned} e_{n,s,t} &= \eta_0 \cdot e_{n,s,t-1} + \eta_{in} |g_{n,s,t}^+| - \eta_{out}^{-1} |g_{n,s,t}^-| \\ &\quad + g_{n,s,t,\text{inflow}} - g_{n,s,t,\text{spillage}} , \\ 0 &\leq e_{n,s,t} \leq E_{n,s} \quad \forall n, s, t . \end{aligned} \quad (10)$$

So far, equations (6) to (10) represent mainly technical constraints but additional constraints can be imposed to bound the solution.

The interconnecting transmission expansion can be limited by a global constraint

$$\sum_{\ell} l_{\ell} \cdot F_{\ell} \leq \text{CAP}_{LV} \quad \leftrightarrow \quad \mu_{LV} , \quad (11)$$

where the sum of transmission capacities F_{ℓ} multiplied by the lengths l_{ℓ} is bounded by a transmission volume cap CAP_{LV} . In this case, the Lagrange/KKT multiplier μ_{LV} represents the shadow price of a marginal increase in transmission volume.

The maximum CO_2 allowed to be emitted by the system CAP_{CO_2} can be imposed through the constraint

$$\sum_{n,s,t} \varepsilon_s \frac{g_{n,s,t}}{\eta_{n,s}} + \sum_{n,s} \varepsilon_s (e_{n,s,t=0} - e_{n,s,t=T}) \leq \text{CAP}_{\text{CO}_2} \quad \leftrightarrow \quad \mu_{\text{CO}_2} \quad (12)$$

where ε_s represents the specific emissions in CO_2 -tonne-per-MWh_{th} of the fuel s , $\eta_{n,s}$ the efficiency and $g_{n,s,t}$ the generators dispatch. In this case, the Lagrange/KKT multiplier represents the shadow price of CO_2 , *i.e.*, the additional price that should be added for every unit of CO_2 to achieve the CO_2 reduction target in an open market.

8. Sectors description and data

8.1. Electricity sector

Hourly electricity demand for every country corresponding to 2015 is retrieved from EU Network Transmission System Operators of Electricity (ENTSO-E) via the convenient dataset prepared by the Open Power System Data (OPSD) initiative [11]. In every country, electricity can be generated by solar PV, onshore wind, offshore wind, Open Cycle Gas Turbines (OCGT), Combined Cycle Gas Turbines (CCGT), coal, lignite, and nuclear power plants and CHP units, with the costs, lifetimes and efficiencies shown in Table 2. Time series representing the hourly capacity factors for solar PV were obtained by converting weather data into solar electricity generation, assuming a uniform capacity layout across every country. Details on the conversion and aggregation methodology can be found in [12], the complete time series dataset is available in [10.5281/zenodo.1321809](https://doi.org/10.5281/zenodo.1321809). CHP units are modelled as extraction condensing units, the feasible space representing the possible combinations of power and heat outputs is included as a constraint in the model, as detailed in [13].

TODO: Describe onshore/offshore time series and maximum capacities.

TODO: Describe maximum capacities.

The transmission links between countries are assumed to be high-voltage direct current (HVDC) connections. For 2020 and 2030, the capacities corresponds to the values assumed in the ENTSOE Ten-Year Network Development Plan (TNYDP), see Table 1 and [14]. The values for 2025 are interpolated assuming

a liner capacity expansion between 2020 and 2030 for every link. For years from 2035 onwards, capacities are optimized together with the rest of the system components using 2030 values as lower boundary. **TODO: Describe other scenarios**

For conventional technologies, *i.e.* OCGT, CCGT, coal, lignite, nuclear and CHP, installed capacities in every country in 2020 and commissioning dates are retrieved from [6]. A two-step method was implemented to fill commissioning date for power plants whose data was missing. First, for units larger than 50 MW, commissioning date has been searched and manually added. Then, for smaller units, a Kernel Density Estimation (KDE) approach is used. *I.e.*, for every technology and country, the units with available data are used to create a distribution, which is then used to assign an estimated commissioning date for those units with missing data. For solar PV, the installed capacities in 2020 and the installation dates were obtained by processing annual installed capacities statistics from [7]. For offshore and onshore wind, capacities and age are retrieved from [15].

TODO: Include figure with the sectors included.

8.2. Heating sector

Annual heat demand for every country are retrieved from [16]. They are converted into hourly heat demand based on the population-weighted [17] Heating Degree Hour (HDH), that is, heating is assumed to be proportional to the difference between ambient temperature and a threshold temperature. 17°C is assumed as threshold temperature. **TODO: Change to daily profiles?** In high-density population areas, heating can be supplied by central heat pumps, heat resistors and gas boilers, as well as by CPH and **solar collectors**. In low-density population areas, heating can be supplied by individual heat pumps, heat resistors and gas boilers. Costs, lifetimes, and efficiencies of the different technologies are included in Table 2.

TODO: Describe temperature-dependent efficiency of heat pumps. Include formula for LCOE estimation. Describe reference and method for existing heating capacities. Describe hypotheses on biomass and assumptions from JRC-ENSURES. Describe path of deployment of district heating. Describe path of electrification of transport.

9. Cost assumptions

Figure 9: Cost evolution assumed for the different technologies.

10. References

- [1] C. Figueres, H. J. Schellnhuber, G. Whiteman, J. Rockström, A. Hobley, S. Rahmstorf, [Three years to safeguard our climate](#), Nature News 546 (7660) 593. doi:10.1038/546593a.
URL <http://www.nature.com/news/three-years-to-safeguard-our-climate-1.22201>
- [2] G. Peters, How much carbon dioxide can we emit?
URL <https://cicero.oslo.no/en/posts/climate/how-much-carbon-dioxide-can-we-emit>
- [3] M. R. Raupach, S. J. Davis, G. P. Peters, R. M. Andrew, J. G. Canadell, P. Ciais, P. Friedlingstein, F. Jotzo, D. P. Vuuren, C. L. Quéré, [Sharing a quota on cumulative carbon emissions](#), Nature Climate Change 4 (10) (2014) 873–879. doi:10.1038/nclimate2384.
URL <https://www.nature.com/articles/nclimate2384>
- [4] National emissions reported to the UNFCCC and to the EU Greenhouse Gas Monitoring Mechanism , EEA.
URL <https://www.eea.europa.eu/data-and-maps/data/national-emissions-reported-to-the-unfccc-and-to-the-eu-greenhouse-gas>
- [5] L. Mantzos, T. Wiesenhal, N. Matei, S. Tchung-Ming, M. Rzsai, H. P. Russ, A. Soria, [JRC-IDEES: Integrated Database of the European Energy Sector](#)doi:10.2760/182725.
URL <http://www.sciencedirect.com/science/article/pii/S0360544216310295>
- [6] powerplantmatching.
URL <https://github.com/FRESNA/powerplantmatching>
- [7] Renewable Capacity Statistics 2019, IRENA.
URL <https://www.irena.org/publications/2019/Mar/Renewable-Capacity-Statistics-2019>

Table 1: Transmission capacities (MW) for interconnections [14].

| Link | 2020 | 2030 | Link | 2020 | 2030 | Link | 2020 | 2030 |
|-------|------|------|-------|------|------|-------|------|------|
| AL-GR | 250 | 250 | FI-EE | 1000 | 1000 | LU-FR | 0 | 0 |
| AL-ME | 350 | 350 | FI-NO | 0 | 0 | LV-EE | 1600 | 1600 |
| AL-MK | 200 | 200 | FI-SE | 2300 | 2800 | LV-LT | 1200 | 1800 |
| AL-RS | 760 | 760 | FR-BE | 4300 | 4300 | ME-AL | 350 | 350 |
| AT-CH | 1700 | 1700 | FR-CH | 3700 | 3700 | ME-BA | 400 | 400 |
| AT-CZ | 1000 | 1000 | FR-DE | 3000 | 4800 | ME-IT | 1200 | 1200 |
| AT-DE | 5000 | 7500 | FR-ES | 5000 | 8000 | ME-RS | 1000 | 1000 |
| AT-HU | 1200 | 1200 | FR-GB | 5400 | 5400 | MK-AL | 200 | 200 |
| AT-IT | 555 | 1655 | FR-IE | 0 | 700 | MK-BG | 150 | 150 |
| AT-SI | 1200 | 1200 | FR-IT | 4350 | 4350 | MK-GR | 400 | 400 |
| BA-HR | 1344 | 1844 | FR-LU | 380 | 380 | MK-RS | 1050 | 1050 |
| BA-ME | 500 | 500 | GB-BE | 1000 | 1000 | NI-GB | 80 | 500 |
| BA-RS | 1100 | 1100 | GB-DK | 1400 | 1400 | NI-IE | 1100 | 1100 |
| BE-DE | 1000 | 1000 | GB-FR | 5400 | 5400 | NL-BE | 2400 | 2400 |
| BE-FR | 2800 | 2800 | GB-IE | 500 | 500 | NL-DE | 4450 | 5000 |
| BE-GB | 1000 | 1000 | GB-IS | 0 | 0 | NL-DK | 700 | 700 |
| BE-LU | 1080 | 1080 | GB-NI | 500 | 500 | NL-GB | 1000 | 1000 |
| BE-NL | 2400 | 2400 | GB-NL | 1000 | 1000 | NL-NO | 700 | 700 |
| BG-GR | 1728 | 1728 | GB-NO | 1400 | 1400 | NO-DE | 1400 | 1400 |
| BG-MK | 530 | 530 | GR-AL | 250 | 250 | NO-DK | 1640 | 1640 |
| BG-RO | 1400 | 1400 | GR-BG | 1032 | 1032 | NO-FI | 0 | 0 |
| BG-RS | 600 | 600 | GR-CY | 2000 | 2000 | NO-GB | 1400 | 1400 |
| CH-AT | 1700 | 1700 | GR-IT | 500 | 500 | NO-NL | 700 | 700 |
| CH-DE | 4700 | 4700 | GR-MK | 350 | 350 | NO-SE | 3695 | 3695 |
| CH-FR | 1300 | 1300 | HR-BA | 1312 | 1812 | PL-CZ | 600 | 600 |
| CH-IT | 6240 | 6240 | HR-HU | 2000 | 2000 | PL-DE | 3000 | 3000 |
| CY-GR | 2000 | 2000 | HR-IT | 0 | 0 | PL-DK | 0 | 0 |
| CZ-AT | 1200 | 1200 | HR-RS | 600 | 600 | PL-LT | 1000 | 1000 |
| CZ-DE | 2100 | 2600 | HR-SI | 2000 | 2000 | PL-PL | 5000 | 5000 |
| CZ-PL | 500 | 500 | HU-AT | 800 | 800 | PL-SE | 600 | 600 |
| CZ-SK | 2100 | 2100 | HU-HR | 2000 | 2000 | PL-SK | 990 | 990 |
| DE-AT | 5000 | 7500 | HU-RO | 1300 | 1300 | PT-ES | 3500 | 3500 |
| DE-BE | 1000 | 1000 | HU-RS | 600 | 600 | RO-BG | 1500 | 1500 |
| DE-CH | 3286 | 3286 | HU-SI | 1700 | 1700 | RO-HU | 1400 | 1400 |
| DE-CZ | 1500 | 2000 | HU-SK | 2000 | 2000 | RO-RS | 1450 | 1450 |
| DE-DK | 4000 | 4000 | IE-FR | 0 | 700 | RS-AL | 330 | 330 |
| DE-FR | 3000 | 4800 | IE-GB | 500 | 500 | RS-BA | 1200 | 1200 |
| DE-LU | 2300 | 2300 | IE-NI | 1100 | 1100 | RS-BG | 350 | 350 |
| DE-NL | 4450 | 5000 | IS-GB | 0 | 0 | RS-HR | 600 | 600 |
| DE-NO | 1400 | 1400 | IT-AT | 385 | 1385 | RS-HU | 600 | 600 |
| DE-PL | 2000 | 2000 | IT-CH | 3860 | 3860 | RS-ME | 1100 | 1100 |
| DE-SE | 615 | 1315 | IT-FR | 2160 | 2160 | RS-MK | 950 | 950 |
| DK-DE | 4000 | 4000 | IT-GR | 500 | 500 | RS-RO | 1050 | 1050 |
| DK-DK | 1200 | 1200 | IT-HR | 0 | 0 | SE-DE | 615 | 1315 |
| DK-GB | 1400 | 1400 | IT-IT | 5750 | 5750 | SE-DK | 1980 | 1980 |
| DK-NL | 700 | 700 | IT-ME | 1200 | 1200 | SE-FI | 2400 | 3200 |
| DK-NO | 1640 | 1640 | IT-SI | 1380 | 1380 | SE-LT | 700 | 700 |
| DK-PL | 0 | 0 | IT-TN | 0 | 0 | SE-NO | 3995 | 3995 |
| DK-SE | 2440 | 2440 | LT-LV | 1500 | 2100 | SE-PL | 600 | 600 |
| EE-FI | 1016 | 1016 | LT-PL | 1000 | 1000 | SI-AT | 1200 | 1200 |
| EE-LV | 1600 | 1600 | LT-SE | 1700 | 700 | SI-HR | 2000 | 2000 |
| ES-FR | 5000 | 8000 | LU-BE | 700 | 700 | SI-HU | 2000 | 2000 |
| ES-PT | 4200 | 4200 | LU-DE | 2300 | 2300 | SI-IT | 1530 | 1530 |

- [8] Photovoltaics Report, Tech. rep., Fraunhofer ISE (2019).
URL <https://www.ise.fraunhofer.de/content/dam/ise/de/documents/publications/studies/Photovoltaics-Report.pdf>
- [9] M. Victoria, C. Gallego, I. Anton, G. Sala, Past, Present and Future of Feed-in Tariffs in Spain: What are their Real Costs?, 27th European Photovoltaic Solar Energy Conference and Exhibition (2012) 4612–4616 [doi:10.4229/27thEUPVSEC2012-6CV.3.49](https://doi.org/10.4229/27thEUPVSEC2012-6CV.3.49).
URL <http://www.eupvsec-proceedings.com/proceedings?paper=17736>
- [10] T. Brown, P. Schierhorn, E. Tröster, T. Ackermann, Optimising the european transmission system for 77% renewable electricity by 2030 10 (1) 3–9. [doi:10.1049/iet-rpg.2015.0135](https://doi.org/10.1049/iet-rpg.2015.0135).
- [11] Open Power System Data. 2018. Data Package Time series. Version 2018-03-13. (Primary data from various sources, for a complete list see URL).
URL https://data.open-power-system-data.org/time_series/2018-03-13/.
- [12] M. Victoria, G. B. Andresen, Using validated reanalysis data to investigate the impact of the PV system configurations at high penetration levels in european countries, Progress in Photovoltaics: Research and Applications 27 (7) 576–592. [doi:10.1002/pip.3126](https://doi.org/10.1002/pip.3126).
URL <https://onlinelibrary.wiley.com/doi/full/10.1002/pip.3126>
- [13] T. Brown, D. Schlachtberger, A. Kies, S. Schramm, M. Greiner, Synergies of sector coupling and transmission reinforcement in a cost-optimised, highly renewable European energy system, Energy 160 (2018) 720–739. [doi:10.1016/j.energy.2018.06.222](https://doi.org/10.1016/j.energy.2018.06.222).
URL <http://www.sciencedirect.com/science/article/pii/S036054421831288X>
- [14] Ten-Year Network Development Plan 2016, ENTSOE.
URL <https://tyndp.entsoe.eu/maps-data/>
- [15] Wind energy database.
URL <https://www.thewindpower.net/>
- [16] Deliverable 3.1: Profile of heating and cooling demand in 2015. Data Annex. Heat Roadmap Europe.
URL www.heatroadmap.eu
- [17] Population density by NUTS 3 region.

Table 2: Cost assumptions per technology and year.

| Technology ¹ | 2020 | 2025 | 2030 | 2035 | 2040 | 2045 | 2050 | source |
|----------------------------|--------|--------|--------|--------|--------|--------|--------|--------|
| Onshore Wind | 985 | 946 | 906 | 888 | 870 | 852 | 834 | |
| Offshore Wind | 1920 | 1780 | 1640 | 1578 | 1515 | 1452 | 1390 | |
| Solar PV (utility-scale) | 617 | 563 | 510 | 486 | 462 | 437 | 413 | |
| Solar PV (rooftop) | 1070 | 949 | 828 | 761 | 694 | 627 | 560 | |
| OCGT | 454 | 445 | 435 | 429 | 424 | 418 | 412 | |
| CCGT | 1300 | 1250 | 1200 | 1175 | 1150 | 1125 | 1100 | |
| Coal | 1900 | 1880 | 1860 | 1841 | 1822 | 1803 | 1784 | |
| Lignite | 1500 | 1500 | 1500 | 1500 | 1500 | 1500 | 1500 | |
| Nuclear | 6000 | 6000 | 6000 | 6000 | 6000 | 6000 | 6000 | |
| Reservoir hydro | 2000 | 2000 | 2000 | 2000 | 2000 | 2000 | 2000 | |
| PHS | 2000 | 2000 | 2000 | 2000 | 2000 | 2000 | 2000 | |
| Hydrogen storage | 0 | 0 | 0 | 0 | 0 | 0 | 0 | |
| Battery storage | 192 | 192 | 192 | 192 | 192 | 192 | 192 | |
| Battery inverter | 411 | 411 | 411 | 411 | 411 | 411 | 411 | |
| Electrolysis | 350 | 350 | 350 | 350 | 350 | 350 | 350 | |
| Fuel cell | 339 | 339 | 339 | 339 | 339 | 339 | 339 | |
| Methanation | 1000 | 1000 | 1000 | 1000 | 1000 | 1000 | 1000 | |
| DAC (direct-air capture) | 250 | 250 | 250 | 250 | 250 | 250 | 250 | |
| Central gas boiler | 63 | 63 | 63 | 63 | 63 | 63 | 63 | |
| Decentral gas boiler | 175 | 175 | 175 | 175 | 175 | 175 | 175 | |
| Central resistive heater | 100 | 100 | 100 | 100 | 100 | 100 | 100 | |
| Decentral resistive heater | 100 | 100 | 100 | 100 | 100 | 100 | 100 | |
| HVDC overhead | 400 | 400 | 400 | 400 | 400 | 400 | 400 | |
| HVDC inverter pair | 150000 | 150000 | 150000 | 150000 | 150000 | 150000 | 150000 | |

¹ Add item.

Table 3: Efficiency, lifetime and FOM cost per technology.

| Technology | FOM ^a [%/a] | Lifetime [a] | Efficiency | Source |
|-------------------------------|---------------------------|-----------------|------------|--------|
| Onshore Wind | 2.4 | 30 | | |
| Offshore Wind | 2.3 | 30 | | |
| Solar PV (utility-scale) | 1.3 | 25 | | |
| Solar PV (rooftop) | 1.2 | 25 | | |
| OCGT | 1.8 | 30 | 0.39 | |
| CCGT | 2.3 | 30 | 0.5 | |
| Coal | 1.6 | 40 | 0.35 | |
| Lignite | 2.0 | 40 | 0.45 | |
| Nuclear | 2.0 | 45 | 0.34 | |
| Reservoir hydro | 1.0 | 80 | 0.9 | |
| PHS | 1.0 | 80 | 0.75 | |
| Hydrogen storage | | 20 | | |
| Battery storage | | 15 | | |
| Battery inverter | 3.0 | 20 | 0.81 | |
| Electrolysis | 4.0 | 18 | 0.8 | |
| Fuel cell | 3.0 | 20 | 0.58 | |
| Methanation | 3.0 | 25 | 0.6 | |
| DAC (direct-air capture) | 4.0 | 30 | | |
| Central gas boiler | 1.0 | 22 | 0.9 | |
| Decentral gas boiler | 2.0 | 20 | 0.9 | |
| Central resistive heater | 2.0 | 20 | 0.9 | |
| Decentral resistive heater | 2.0 | 20 | 0.9 | |
| Combined Heat and Power | | | | |
| Central water tank | | | | |
| Decentral water tank | | | | |
| Water tank charger/discharger | | | 0.9 | |
| HVDC overhead | 2.0 | 40 | | |
| HVDC inverter pair | 2.0 | 40 | | |

^a Fixed Operation and Maintenance (FOM) costs are given as a percentage of the overnight cost per year.

URL <https://data.europa.eu>